Bipedal Gait Like Motions of a Thin Viscoelastic Object

Ixchel G. Ramirez-Alpizar, Mitsuru Higashimori, and Makoto Kaneko
Department of Mechanical Engineering, Graduate School of Engineering, Osaka University
2-1 Yamadaoka, Suita, 565-0871, Japan
Email: ixchel@hh.mech.eng.osaka-u.ac.jp, higashi@mech.eng.osaka-u.ac.jp, mk@mech.eng.osaka-u.ac.jp

***Abstract*— This paper discusses a dynamic nonprehensile manipulation of a thin deformable object and its rotational behavior similarity to bipedal gaits toward an effective rotation. A rigid plate end-effector at the tip of a high-speed manipulator can remotely manipulate an object without grasping it. We make use of a simulation model in order to approximate the dynamic characteristics of a thin deformable object on a plate. In this simulation model, we used the parameters estimated from a slice of cheese, as a sample of a real deformable object. Through simulation analysis we show how the object changes its rotational behavior with an analogy to the motion of bipedal gaits sliding, walking, and running. We investigate how the friction between the plate and the object influences the object's angular velocity. We show that an optimum friction point exists and that it is determined based on the object's rotational behavior.**

I. Introduction

Along with the advance of technology in both sensing and actuation, various types of dynamic skills in robotics have been developed. In the case where a simple end-effector is used, a robot-system can compensate for its lack of DOFs (degrees of freedom) by utilizing dynamic effects produced by high-speed robot motions and by using an appropriate manipulation strategy. There have been various works discussing nonprehensile manipulation [1]–[7], among others, including our former work [7]. In which we proposed a dynamic manipulation inspired by the handling of a pizza peel . A chef handles the peel and remotely manipulates a pizza on the plate. We found that the chef aggressively utilizes two DOFs from the remote handling location during the manipulation: translation X along the bar and rotation Θ around the bar, as shown in Fig. 1(a). This manipulation scheme has the advantage that the robot can remotely manipulate an object in areas with high temperatures, electromagnetic fields, etc, where electrical hardware is unavailable. We have proposed a dynamic nonprehensile manipulation for controlling the position and the orientation of an object on a plate by applying the peel mechanism to the robot system.

Most of the works done on manipulation utilizing a plate have supposed that the object is rigid not deformable. Thus, we have also proposed a dynamic nonprehensile manipulation for a deformable object, in which we have found that a deformable object can rotate faster than a rigid one [8], as shown in Fig. 1(b). We have also found that there exists and optimum plate motion leading to the maximal angular velocity of the deformable object. In order to extend the aforementioned investigation, in this paper we investigate the influence that the friction between the plate and the object has in the object's angular velocity and its relation with the object's behavior of rotation.

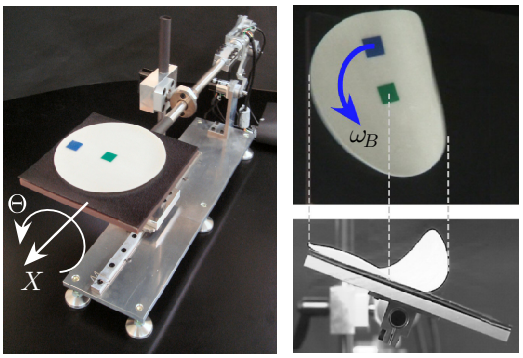

(a) (b)

Fig. 1. Nonprehensile manipulation for rotating an object: overview of the experimental system in (a) and the rotational behavior of a deformable object in (b).

In this paper, after explaining the principle of rotation, we briefly review the simulation model used to approximate the dynamic characteristics of a thin deformable object on the plate. Through simulation analysis, we first show that the object's rotational behavior changes with respect to the plate's motion frequency, similar to sliding, walking, and running gaits done by bipeds. Then, we investigate how the friction between the plate and the object influences the object's angular velocity and show that the optimum friction point is determined based on the object's rotational behavior.

This paper is organized as follows. In section II, we explain the essence of the principle of rotation. In section III, we review the simulation model for a deformable object. In section IV, we show the simulation analysis based on real food. In section V, we give the conclusion of this work.

II. Principle of Rotation

Let us briefly explain the principle of rotation that we will use later in Section IV. Fig. 2 shows the top view and the side view of the object on the plate, this plate has two DOFs: translation X along the bar and rotation Θ around the bar,

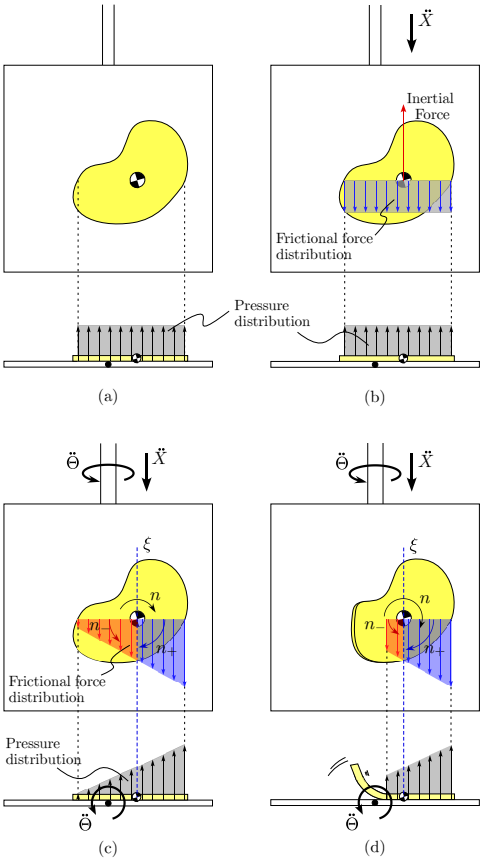

Fig. 2. Mechanism for rotating an object on the plate

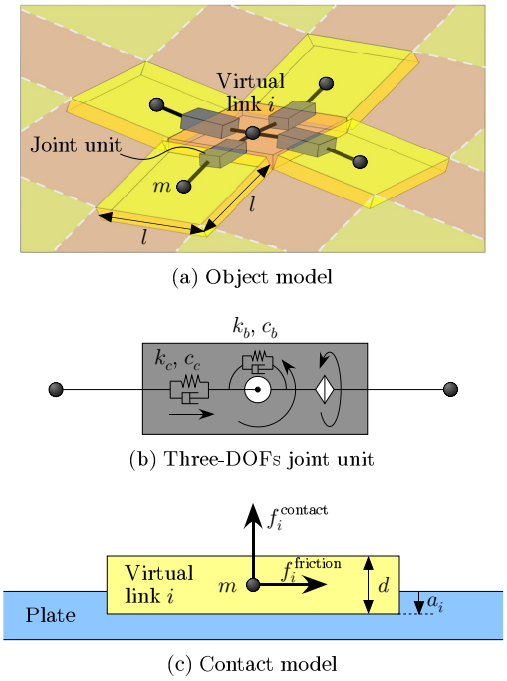

Fig. 3. Deformable object model.

as shown in Fig. 1(a). The object as well as the plate are stationary ($X = 0$, $\Theta = 0$) in Fig. 2(a). Then, as shown in Fig. 2(b), by giving a translational acceleration $\ddot{X}$ to the plate, an inertial force and a frictional force are generated. In this case the nominal pressure distribution on the object is assumed to be uniform and as a result the frictional force distribution is also uniform, as shown in Fig. 2(b), where we illustrate just the slice of the frictional force distribution that passes through the center of mass of the object.Let us now consider the case in which an angular acceleration $\ddot{\Theta}$ is additionally given to the plate, as shown in Fig. 2(c). In this instance, the pressure distribution on the object results in a slope due to the inertial force generated by $\ddot{\Theta}$, thus the frictional force distribution also slopes. A rotational moment n around the object's center of mass is generated by the slope in the frictional force, and therefore the object rotates. Let us consider that a line ξ which passes through the object's center of mass and runs parallel to the translational motion $\ddot{X}$, divides the rotational moment n into the moment contributing to rotation n_+ and the moment braking rotation n_-. In the case of a deformable object, as shown in Fig. 2(d), the inertial force generated by the plate's rotational motion produces a deformation in the object and as a result, the object's area in contact with the plate is reduced. Hence the moment braking rotation n_- decreases. From this reason it is thought that a deformable object rotates faster than a rigid one.

III. Simulation Model

In preparation for the motion analysis we briefly review the viscoelastic model for approximating dynamic behaviors of a thin deformable object on a plate.

Assumptions: Consider a plate and a thin deformable object as shown in Fig. 1(a). To simplify the analysis, we set the following assumptions:

1: The plate is rigid.
2: The plate's surface area is larger than that of the object.
3: The object is deformable and its thickness is small.
4: The object is isotropic and it has uniform mass distribution and uniform viscoelasticity.
5: The nominal pressure distribution on the object is uniform.
6: The friction coefficient between the plate and the object based on Coulomb's law is uniform and is given by μ_s and μ_k for static and dynamic coefficients, respectively.

Deformable object model: For a thin deformable object, as introduced in [8], we consider virtual tile links as shown in Fig. 3(a). The link is a square with sides of length l. A node with a mass of m is located at the center of the link, where neighboring nodes are connected to each other by a viscoelastic joint unit as shown in Fig. 3(b). The joint unit is composed of three DOFs: bending, compression/tension, and torsion. Where the bending and the compression joints have

viscoelastic elements given by a Kelvin-Voigt model, where k_b and c_b express the elasticity and viscosity, respectively, of the bending joint and k_c and c_c express the elasticity and viscosity, respectively, of the compression joint. The torsion joint is free for simplicity of the simulation model.

Contact Model: Fig. 3(c) shows the contact model between the plate and the i-th virtual link. The contact force is computed with the penalty method based on the Kelvin-Voigt model [9]. The contact force f_i^{contact} applied to the node is given by

$$f_i^{\text{contact}} = k_{\text{contact}} a_i^{2.2} + c_{\text{contact}} \dot{a}_i \quad (a_i \geq 0) \qquad (1)$$

where a_i, k_{contact}, and c_{contact} are the distance between the surface of the plate and that of the virtual link, the elasticity, and the viscosity, respectively. Also, the frictional force f_i^{friction} applied to the node is given by,

$$f_i^{\text{friction}} = \mu f_i^{\text{contact}} \quad (\mu = \mu_k \text{ or } \mu_s) \qquad (2)$$

where f_i^{friction} is in the opposite direction to the relative velocity of the node with respect to the plate's surface.

Parameters of the Model: As introduced and explained in [8], the viscoelastic parameters in bending and compression were estimated using a slice of cheese since it is an artificial product that can reasonably correspond to assumptions 4, 5, and 6. Based on the model shown in Fig. 3(a), each squared link has a length of $l = 10$ mm, thickness $d = 2.5$ mm, and mass $m = 0.285$ g. For the bending joint the viscoelastic parameters were obtained as: $\hat{k}_b = 2.72 \times 10^{-3}$ N·mm/deg and $\hat{c}_b = 4.23 \times 10^{-6}$ N·mm/(deg/s). And for the compression joint the viscoelastic parameters were obtained as: $\hat{k}_c = 0.79$ N/mm and $\hat{c}_c = 4.9 \times 10^{-4}$ N/(mm/s).

IV. Simulation Analysis

We investigate through simulation analysis, how the object's behavior changes with respect to the given plate motion and show that there exists an optimum friction point that yields the maximal angular velocity of the object.

A. Settings

A commercially available slice of cheese is used for simulation analysis. The slice of cheese has a circular shape of radius $r = 40$ mm, thickness $d = 2.5$ mm, and mass $M = 13.6$ g. The simulation software MD Adams (MSC.Software Corp.) is utilized to compute the dynamic motion of the object. The simulation model as shown in Fig. 3(a) is composed of 52 links with $l = 10$ mm. The four viscoelastic parameters given in the previous section are utilized together with the friction's coefficients $\mu_s = 0.75$ and $\mu_k = 0.4$ obtained experimentally. Additionally, $k_{\text{contact}} = 11.86$ N/mm, $c_{\text{contact}} = 7.65 \times 10^{-3}$ N/(mm/s) are given. In order to rotate the object, we give to the plate's two DOFs of motion the following sinusoid trajectories

$$\Theta(t) = -A_p \sin(\omega_p t) \qquad (3)$$

$$X(t) = B_p \sin(\omega_p t) \qquad (4)$$

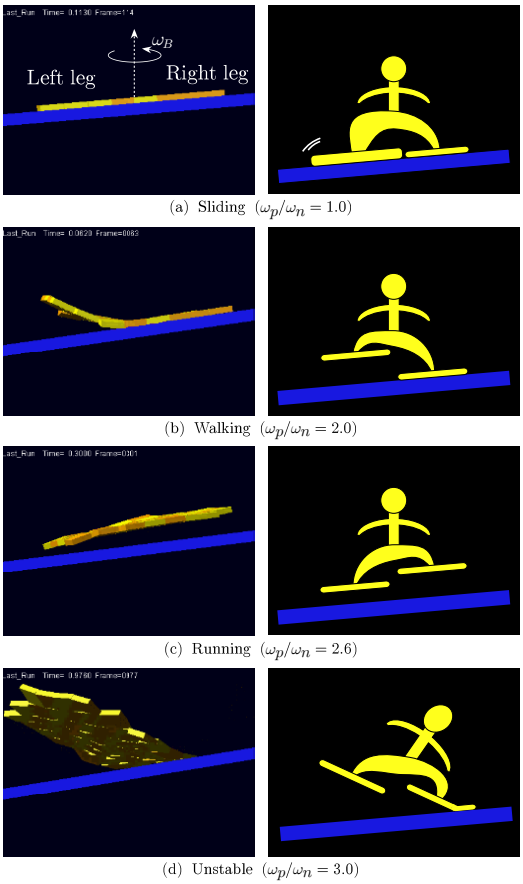

(a) Sliding $(\omega_p/\omega_n = 1.0)$

(b) Walking $(\omega_p/\omega_n = 2.0)$

(c) Running $(\omega_p/\omega_n = 2.6)$

(d) Unstable $(\omega_p/\omega_n = 3.0)$

Fig. 4. Analogy to bipedal gaits

where A_p, B_p, and ω_p denote the rotational amplitude, the linear amplitude, and the angular frequency of the plate motion, respectively.

B. Analogy to Bipedal Gaits

In the simulation of a slice of cheese, with $A_p = 12$ deg, $B_p = 3$ mm, and $\omega_p = 12 \times 2\pi$ rad/s, it can be noted that the object's behavior changes with respect to ω_p, as shown in Fig. 4, where ω_p is normalized by $\omega_n = 10\pi$ rad/s which is the first order natural angular frequency of the object in bending. An interesting observation is that, if the whole object is separated into two parts by its center, as shown in Fig. 4(a), and regarding each of these parts as left leg and right leg; then the object's behavior can be described with an analogy to bipedal gaits as follows: sliding (both legs always make contact with the floor), as shown in Fig. 4(a), walking (at least one leg makes contact with the floor), as shown in Fig. 4(b), and running (both legs float at the same time), as shown in Fig. 4(c). Finally, for a larger ω_p, the object becomes unstable and it cannot rotate anymore, as shown in Fig. 4(d). We define failures as those cases in which the object's center slips more than 10 mm or when the object turns over.

C. Optimum Friction Point

The simulation results in Fig. 5 show the relationship between the angular acceleration of the plate $A_p\omega_p^2$, the friction angle between the plate and the object $\alpha = \tan^{-1}(\mu_s)$ and the angular velocity of the object ω_B, for a plate's rotational amplitude $A_p = 3$ deg, translational amplitude $B_p = 3$ mm and $\omega_n = 10\pi$ rad/s. The □, △, and ◯ denote the object's sliding, walking, and running phases, respectively. Here, it must be pointed out that not only the static coefficient of friction μ_s, but also the dynamic coefficient of friction μ_k changes and it does it proportionally to μ_s, that is $\mu_k = \beta\mu_s$, where $\beta = 0.53$ is constant.

The friction's influence in the object's angular velocity ω_B, as shown in Fig. 5, can also be explained with the analogy to bipedal gaits. When the friction angle α is around 0 deg, the object cannot rotate fast because the moment contributing to rotation n_+ cannot be generated. This corresponds with a slippery floor for a biped's gait. In the other extreme, when the friction angle α is around 80 deg, the object also cannot rotate fast because the frictional force becomes too large so that it almost reaches a balance with the inertial force, i.e. it is very close to neutralize the inertial force thus the rotational moment generated is small. This corresponds with a sticky floor, where a biped can hardly step. Thus the optimum friction angle leading to the maximal angular velocity $\omega_{B\max}$ exists in an intermediate friction value. For a small $A_p\omega_p^2$ as in the sliding phase □, the object keeps full contact with the plate and no deformation occurs. In this case, both the contributing moment n_+ and the braking moment n_- are generated, as shown in Fig. 2(c), and the optimum friction angle is around 40 deg. In the walking phase △, the braking moment n_- decreases due to the object's deformation, as explained in Fig. 2(d). Therefore the optimum friction angle moves to a larger one, around 60 deg, so as to increase the contributing moment n_+ without overcoming the inertial force. For a larger $A_p\omega_p^2$ as in the running phase ◯, the object's contact area during rotation is drastically reduced. Thus the object rotates faster by the inertial effect while floating on the air for most of the time, without making contact with the plate. In this case, a large friction brakes the object's rotation at the instants of time it makes contact with the plate. To avoid this braking, the optimum friction angle moves to a smaller one, around 30 deg. As it was explained, the optimum friction point denoted by arrows in Fig. 5, depends on the object's rotational behaviors of sliding, walking, and running.

Furthermore, the optimum angular acceleration $A_p\omega_p^2$ is obtained around 8 deg/s^2, regardless of the friction angle α. This suggests that an appropriate plate's angular acceleration is the most essential point for a fast object's rotation.

V. Conclusion

This paper discussed a dynamic nonprehensile manipulation strategy for rotating a thin viscoelastic object on a rigid two DOFs plate. The main results of this paper are summarized as follows:

- We showed through simulation analysis that the transition of the object's rotational behavior with respect to the plate frequency, mimics either a sliding, walking, or running gait of a biped.
- We showed that the optimum friction between the plate and the object, which leads to the maximal rotational velocity of the object, is determined based on the object's rotational behavior.
- We showed that the plate's optimum angular acceleration is determined regardless of the friction value between the plate and the object.

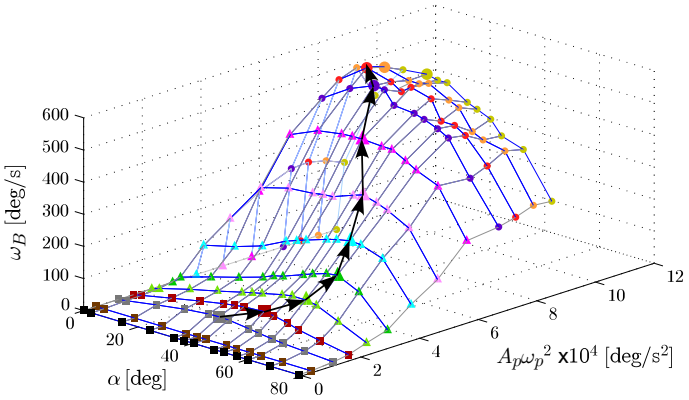

Fig. 5. Relationship between the friction angle between the plate and the object α, the angular acceleration of the plate $A_p\omega_p^2$, and the angular velocity of the object ω_B

References

[1] H. Arai and O. Khatib: "Experiments with Dynamic Skills," Proc. of 1994 Japan-USA Symp. on Flexible Automation, pp.81–84, 1994.

[2] K. M. Lynch and M. T. Mason: Dynamic Nonprehensile Manipulation: Controllability, Planning, and Experiments, Int. J. of Robotics Research, vol.18, no.8, pp.64–92, 1999.

[3] A. Amagai and K. Takase: "Implementation of Dynamic Manipulation with Visual Feedback and Its Application to Pick and Place Task," Proc. of the IEEE Int. Symp. on Assembly and Task Planning, pp.344–350, 2001.

[4] D. Reznik and J. Canny: "C'mon Part, Do the Local Motion!," In IEEE Proc. of the IEEE Int. Conf. on Robotics and Automation, pp.2235–2242, 2001.

[5] K. F. Böhringer, V. Bhatt, and K. Goldberg: Sensorless Manipulation Using Transverse Vibrations of a Plate, Proc. of the IEEE Int. Conf. on Robotics and Automation, pp.1989–1986, 1995.

[6] T. Vose, P. Umbanhowar, and K. M. Lynch, "Friction-induced velocity fields for point parts sliding on a rigid oscillated plate," Int. J. of Robotics Research, vol. 28, no. 8, pp. 1020–1039, Aug. 2009.

[7] M. Higashimori, K. Utsumi, Y. Omoto, and M. Kaneko: "Dynamic Manipulation Inspired by the Handling of a Pizza Peel," IEEE Transactions on Robotics, vol.25, no.4, pp.829–838, 2009.

[8] I. G. Ramirez-Alpizar, M. Higashimori, M. Kaneko, C. Tsai and I. Kao, "Nonprehensile dynamic manipulation of a sheet-like viscoelastic object," Proc. of the IEEE Int. Conf. on Robotics and Automation, Shanghai, China, 2011, pp. 5103–5108.

[9] M. Moore, and J. Wihelms: "Collision Detection and Response for Computer Animation," Computer Graphics, vol.22, no.4, pp.289–298, 1988.